THE THEORY OF LOCAL ADVECTION: I

By J. R. Philip

California Institute of Technology,[1] Pasadena; and Commonwealth Scientific and Industrial Research Organization, Australia[2]

(Manuscript received 26 November 1958)

ABSTRACT

This paper is the first of a series in which the theory of local advection (the exchange due to horizontal heterogeneity) of energy and moisture will be developed and applied to a number of problems of practical and theoretical interest. The paper provides an introduction to the practical implications and physical basis of local advection, but it is mainly devoted to developing methods of analysis to be applied in later papers. The treatment aims to provide simple and rapid numerical procedures for the solution of advection problems.

Methods are given for solving the two-dimensional atmospheric-diffusion equation subject to "concentration," "flux," and "radiation" types of boundary conditions. Appendices give discussions of the properties of the functions entering the solutions and provide simple means for their computation. Extensive tables of the relevant functions are given for the case $m = 1/7$, $n = 6/7$ (m, n being the exponents in the power-law approximations to the vertical profiles of mean wind speed and eddy diffusivity, respectively).

The rudiments of a quantitative theory of advective inversion are developed, expressions being obtained for the equation of the inversion surface, and for the maximum height and downwind extent of the inversion.

1. Introduction

In this real world, irrigated fields adjoin deserts, reservoirs are of finite extent, dry lands exist beside seas, and cornfields beside close-grazed pasture. It is not surprising, then, that many important problems of micrometeorology require that we take cognizance of *advection*. This we define as the exchange of energy, moisture, or momentum due to horizontal heterogeneity. One symptom of the presence of advection is that vertical mean profiles of (potential) temperature, specific humidity, and wind speed are non-equilibrium profiles, even under conditions steady in time.

However, most attempts at quantitative studies in micrometeorology have been based on the assumption of horizontal homogeneity and equilibrium profiles. The possibility of advection has been recognized mainly in a negative way. Experimenters attempt to avoid it by working on sites downwind of extensive "homogeneous" areas. Sometimes advection is invoked to explain otherwise inexplicable observations, but this tends to be a last resort.

The situation has been worse in fields of applied micrometeorology (such as agronomy, ecology, reservoir engineering, irrigation engineering), where neglect or ignorance of the importance of advection has often led to experiments, interpretations, and methods of prediction and design which have not achieved the intended goals.

In particular, the neglect of advection has tended to vitiate many attempts to treat the problem of natural evaporation. There is a logical flaw in treating the humidity and temperature of the air solely as the *cause* of evaporation at the underlying surface. They are equally the *consequences* of the upwind evaporation and energy conditions. [Compare Priestley, 1951; Deacon *et al.*, 1958].

The present study deals with the advection of heat and moisture. It bears on such problems of practical importance and theoretical interest as (i) the influence of the size of an irrigated area and of position within the area on evapotranspiration, (ii) the influence of reservoir size on evaporation losses, (iii) the effect of the presence of an irrigation area and/or a body of water on the microclimate above and downwind of such regions, (iv) the physical basis of advective dewfall, (v) the theory of advective inversion, (vi) quantitative analysis of the errors introduced into micrometeorological (equilibrium) studies by advective effects.

Our problem is, essentially, to solve simultaneously for the temperature and humidity diffusion fields in the lower atmosphere, subject to boundary conditions upwind and at the surface of the region considered. These conditions must be such that the energy balance at the surface is satisfied.

In this first paper of the present study, we discuss the basic physical theory and provide the mathe-

[1] Temporary affiliation, 1958. This work was supported in part by a grant from the Rockefeller Foundation RF 56160.

[2] Permanent address: Division of Plant Industry, Canberra, A.C.T. Part of the analysis presented in this paper was developed by the author during 1956–57 while he was with the Division of Plant Industry, Deniliquin, N.S.W.

matical apparatus which enables us, in later papers, to investigate the various practical and theoretical aspects of advection noted above.

2. Symbolism

a: constant introduced in (36), and evaluated in (47).
A (cal cm^{-2} sec^{-1}): sensible heat exchange between surface and air, positive upward.
b: constant introduced in (39), and evaluated in (48).
c: quantity defined by (45).
$C_m(\eta)$: function of η defined by (17).
E (cm sec^{-1}): evaporation rate.
$f_1(\alpha)$: function of α defined by (51).
$f_2(x)$: function of x defined by (52).
$\mathrm{F}(\eta, \beta)$: function of η defined by (34).

$$F_m(\eta):\ F\left(\eta, 2 + \frac{1}{m}\right).$$

$$I(\eta, p):\ \int_0^\eta e^{-t}t^p dt \Big/ \int_0^\infty e^{-t}t^p dt.$$

K (cm^2 sec^{-1}): eddy diffusivity.
K_1: constant in equation (4).
L (cal g^{-1}): latent heat of evaporation of water (≈ 585).
m: exponent in equation (3).
n: exponent in equation (4).
Q (cal cm^{-2} sec^{-1}): soil heat-flux density at the surface, positive upwards. At water surfaces, the net energy exchange (by conduction, radiation, and convection) between the surface and the underlying body of water, again positive upwards.
r: reflection coefficient of surface for shortwave radiation.
R_a (cal cm^{-2} sec^{-1}): flux density of atmospheric (long-wave) radiation received at the surface.
R_s (cal cm^{-2} sec^{-1}): flux density of short-wave radiation received at the surface.
$T_0(K)$: surface temperature.
u (cm sec^{-1}): mean wind speed.
u_1: constant in equation (3).
x(cm): horizontal coordinate, positive in downwind direction.
$\bar{x}$ (cm): geometrical mean value of x in x-range of interest.
x_1 (cm): value of x at which integrated error in matching boundary condition is zero.
$x_{\max}$ (cm): maximum downwind extent of advective inversion.
X: quantity defined by (38).
$\bar{X}$: value of X for $x = \bar{x}$.
z (cm): vertical co-ordinate, positive upwards, zero at surface.
$z_{\max}$ (cm): maximum height of advective inversion.
α: constant entering radiation-type boundary conditions (9).
β: constant defined by (69).
γ: constant defined by (46).

$$\Gamma(p + 1):\ \int_0^\infty e^{-t}t^p dt.$$

$\Delta_z\theta$: difference in θ (over upwind regions) between $z = 0$ and $z = 10^4$, positive when θ at $z = 0$ is the greater.
$\Delta\theta_0$: difference in θ_0 between upwind and downwind regions, positive when the upwind value is the greater.
ϵ: emissivity of surface (long-wave radiation).
ζ: dimensionless quantity defined in (62).
η: dimensionless quantity defined in (10).
θ: concentration of diffusing entity.[3]
θ_0: value of θ at $z = 0$.
ρ_w (g cm^{-3}): density of liquid water (≈ 1.0).
σ (cal sec^{-1} cm^{-2} K^{-4}): Stefan-Boltzmann constant ($= 1.36 \times 10^{-12}$).
ϕ: flux density of diffusing entity.[3]
ϕ_0: value of ϕ at $z = 0$.
ϕ_{00}: value of ϕ over upwind region.
χ: dimensionless quantity defined in (63).

3. The energy balance: the physical background to advection

At any point at the lower boundary of the atmosphere, the instantaneous energy balance may be written

$$(1 - r)R_s + R_a - \epsilon\sigma T_0^4 + Q = A + L\rho_w E. \quad (1)$$

Usually, we shall be applying (1) to land surfaces, but the equation holds also at water surfaces as long as we redefine Q to denote the net energy exchange (by conduction, radiation, and convection) between the water surface and the underlying body of water.

Evidently, if any one of the quantities entering (1) differs between any two surface points in the same vicinity, at least one (and often more than one) other component of the energy balance will also differ between the points. See Philip (1957) for an elementary treatment of the partition of energy at freely and imperfectly evaporating surfaces.

These horizontal differences in the energy balance occur both in nature and as a result of man's artifice. They may originate from a change in the energy fluxes to the surface due to causes external to the surface, or they may arise from differences in the thermal or radiative properties of the surface, or they may result from differences in the availability of water.

It is of interest to consider ways in which such differences can originate through the various quantities entering (1).

[3] Units of θ and ϕ depend on nature of diffusing entity, and are therefore omitted here.

r, ϵ: The albedo and the emissivity at the two points may differ either naturally (differences in vegetation, soil color, snow cover) or artificially.

R_s, R_a: Horizontal changes in received radiation may arise due to shading by clouds, trees, mountains, and artificial constructions. Such effects may be of short time duration or may be attended by other complications which put them beyond the scope of the present study. An equally important cause of horizontal differences in received radiation, and one which is more amenable to analysis by the present approach, is that due to change of slope of the ground surface (usually natural, but possibly artificial). It will be understood that we shall not be concerned here with points so far apart that their R_s-values differ significantly for astronomical reasons.

Q: In principle, the heat flux of the soil may differ due to horizontal variation in thermal properties of the soil. This seems unlikely to be a major cause of advective effects. A more interesting case arises where a water surface adjoins land. Here the Q-differences may be a dominant factor.

A, E: Horizontal differences in both A and E may be caused by horizontal differences in the intensities of turbulent exchange. Such differences may arise from (natural or artificial) changes in surface roughness. Where wind structure changes markedly, this aspect will be outside the scope of the present treatment.

E: It will be apparent from the later developments that the most common effect of importance arises from differences, either natural or artificial, in the availability of water for evaporation at the surface. It is to this effect that we shall give most attention.

For the sake of completeness, we note that artificial releases of heat should be recognized as a further source of horizontal heterogeneity. Heat production by industries and cities can be regarded as accidental instances while, under some circumstances, the use of oil burners in frost-threatened orchards represents a more intentional production of advective effects. The present approach has only limited application to these problems because there are often other complicating factors.

4. Advection and two-dimensional atmospheric diffusion

In this study, we shall deal only with two-dimensional problems; that is, we assume that cross-wind diffusion may be neglected. Practical application of the theory is therefore limited to regions where the cross-wind dimension is not too small.

The theory to be developed here uses the mathematics of atmospheric diffusion. Certain of the results we use are well known, but others are new. It has seemed to the present author that application of the mathematical theory and, indeed, a feeling for the general character and significance of the results requires that solutions be readily available in numerical form. With Lord Kelvin, we feel that "When you cannot express it in numbers, your knowledge is of a meagre and unsatisfactory kind." Accordingly, the present treatment aims to provide numerical values of the functions entering the solutions and to supply simple and rapid numerical procedures for finding solutions to the problems discussed. In later papers, we shall illustrate various aspects of the theory which seem of interest and significance by means of numerical examples.

The equation which concerns us is

$$u\frac{\partial\theta}{\partial x} = \frac{\partial}{\partial z}\left(K\frac{\partial\theta}{\partial z}\right) \tag{2}$$ [4]

with

$$u = u_1 z^m \tag{3}$$

and

$$K = K_1 z^n. \tag{4}$$

We shall be dealing with three basic types of boundary conditions. The first, which we designate the *concentration* type, is of the general form conveniently represented by (5):

$$\left.\begin{array}{lll} x = 0, & z > 0, & \theta = 0 \\ x \geqslant 0, & z = 0, & \theta = \theta_0(x) \end{array}\right\}. \tag{5}$$

Because linear superposition holds, it will be sufficient for us to consider here the solution only for

$$\left.\begin{array}{lll} x = 0, & z > 0, & \theta = 0 \\ x \geqslant 0, & z = 0, & \theta = 1 \end{array}\right\}. \tag{6}$$

We designate the second type of boundary condition the *flux* type. This may be expressed in the following general form:

$$\left.\begin{array}{lll} x = 0, & z > 0, & \theta = 0 \\ x \geqslant 0, & z = 0, & \phi = \phi_0(x) \end{array}\right\}. \tag{7}$$

Here, ϕ, the flux density, is equal to $-K\partial\theta/\partial z$, so that $\phi_0 = \lim_{z\to 0}(-K\partial\theta/\partial z)$. Because linear superposition holds here also, it is sufficient for us to consider the solution only for

$$\left.\begin{array}{lll} x = 0, & z > 0, & \theta = 0 \\ x \geqslant 0, & z = 0, & \phi = 1 \end{array}\right\}. \tag{8}$$

The third type of boundary condition is a special case of mixed boundary condition, known as the *radiation* type (Carslaw and Jaeger, 1947, p. 13),

[4] Equation (2) is, of course, for conditions steady in time and neglects downwind diffusion, as is customary. It is hoped to examine the significance of the downwind diffusion term in some detail in a later communication.

which involves a linear combination of concentration and flux conditions at $x \geqslant 0$, $z = 0$. We shall deal primarily with the form

$$\left.\begin{aligned} &x = 0, \quad z > 0, \quad \theta = 0 \\ &x \geqslant 0, \quad z = 0, \quad \alpha\theta + (1-\alpha)\phi = 1 \end{aligned}\right\}. \tag{9}$$

We develop the required solutions in the following sections 5 through 7. Note that the analysis is valid for m, n quite general, apart from certain mild restrictions on m and n, which we indicate. However, it is convenient in micrometeorological work to give particular attention to the case $n = 1 - m$, which is consistent with the assumption that the diffusivities for momentum and for the diffusing entity vary in a similar manner with z in that zone of the lower atmosphere in which the shearing stress is virtually constant ("Schmidt's conjugate power law"). Accordingly, we shall give the most important results not only in the form with m and n general, but also for the case $n = 1 - m$. Furthermore, it is of interest to assign a numerical value to m (in the case $n = 1 - m$) so that we gain some insight into the forms our solutions take. Therefore, we shall also present these results in the particular form for $m = 1/7$, a value appropriate to conditions of near-neutral stability (*cf.* Calder 1949, Sutton 1953, p. 238), and of relevance to the problems we later investigate.

We distinguish results for $n = 1 - m$ by the letter A and results for $m = 1/7$ by the letter B. Thus, equation (10) is a general result; (10A) is the particular form of (10) for $n = 1 - m$; (10B) is the particular form of (10A) for $m = 1/7$.

5. Two dimensional diffusion: concentration boundary condition

The solution of (2), (3), and (4) subject to (6) is well known. It is most simply found by introducing the substitutions:

$$\eta = \frac{u_1}{(2+m-n)^2 K_1} \cdot \frac{z^{2+m-n}}{x} \tag{10}$$

$$\eta = \frac{u_1}{(1+2m)^2 K_1} \cdot \frac{z^{1+2m}}{x} \tag{10A}$$

$$\eta = \frac{49 u_1}{81 K_1} \cdot \frac{z^{9/7}}{x}. \tag{10B}$$

This enables reduction of (2), (3), and (4) to[5]

$$\frac{d^2\theta}{d\eta^2} + \frac{d\theta}{d\eta}\left[1 + \frac{1+m}{2+m-n}\eta^{-1}\right] = 0, \tag{11}$$

provided that

$$2 + m - n > 0, \tag{12}$$

so that conditions (6) reduce to

$$\eta = 0, \quad \theta = 1; \qquad \eta \to \infty, \quad \theta \to 0. \tag{13}$$

The micrometeorologically possible values of m and n are such that (12) will always be satisfied.

A first integration of (11) with respect to η yields

$$\frac{d\theta}{d\eta} = B\eta^{-(1+m)/(2+m-n)} e^{-\eta} \tag{14}$$

with B a constant of integration. A second integration and use of conditions (13) give

$$\theta = 1 - \frac{\int_0^\eta \eta^{-(1+m)/(2+m-n)} e^{-\eta} d\eta}{\int_0^\infty \eta^{-(1+m)/(2+m-n)} e^{-\eta} d\eta}; \tag{15}$$

i.e.,

$$\theta = 1 - I\left(\eta, -\frac{1+m}{2+m-n}\right) \tag{16}$$

$$\theta = 1 - I\left(\eta, -\frac{1+m}{1+2m}\right) \tag{16A^6}$$

$$\theta = 1 - I(\eta, -8/9). \tag{16B}$$

Here, $I(\eta, p)$ is the form of the incomplete gamma function given by Pearson (1951).

$$I[\eta, -(1+m)/(2+m-n)]$$

does not exist for $(1+m)/(2+m-n) \geqslant 1$—*i.e.*, for $n \geqslant 1$. It follows that our solution holds only for $n < 1$.[7] In practice, this is a somewhat more restrictive condition than (12) is, but we are still able to represent the $K(z)$ profiles observed in nature to reasonable accuracy.

Unfortunately, the tabulations presented by Pearson are not suitable for micrometeorological purposes. The author has found it simpler to compute the necessary functions *ab initio* than to use Pearson's tables. The properties of (what is essentially) the I-function, and its computation, are treated in Appendix 1. $C_{1/7}[= 1 - I(\eta, -8/9)]$ is tabulated in table 1 and graphed in figs. 4 and 5.

For the case $n = 1 - m$, it is convenient to introduce the function C_m, defined by the following

---

[5] Similarity substitutions effectively reduce the number of independent variables in a given partial differential equation only when the variables removed from the equation by the substitution are also removed from the governing conditions by the same substitution.

That is, the η-substitution may be usefully applied to (2, 3, 4) only when the governing conditions are expressible in terms of η and θ only, as they are here.

Curiously enough, this rather obvious principle does not seem to appear explicitly in the literature, and it is often misunderstood.

[6] Pasquill (1943), Calder (1949), and Sutton (1953, p. 306), give very complicated expressions which may be shown to be equivalent to our much simpler (16A) by use of the following identity (Whittaker and Watson, 1927, p. 239):

$$\Gamma(p) \cdot \Gamma(1-p) = \pi/\sin \pi p.$$

[7] In Yih (1952), this condition is misprinted $n > 1$.

TABLE 1. The functions $C_{1/7}$ and $F_{1/7}$.

η	$C_{1/7}$	$F_{1/7}$
0	1. 000 000	1. 000 000
10^{-12}	0. 950 985	0. 949 975
10^{-11}	936 694	935 390
10^{-10}	918 237	916 555
10^{-9}	894 400	892 224
10^{-8}	863 612	860 802
10^{-7}	823 848	820 219
10^{-6}	772 491	767 804
2×10^{-6}	754 276	749 215
4×10^{-6}	734 604	729 137
6×10^{-6}	722 374	716 655
8×10^{-6}	713 356	707 452
10^{-5}	706 161	700 108
2×10^{-5}	682 636	676 100
4×10^{-5}	657 229	650 171
6×10^{-5}	641 434	634 053
8×10^{-5}	629 788	622 169
0.0001	620 495	612 686
0.0002	590 116	581 689
0.0003	571 232	562 424
0.0004	557 310	548 222
0.0005	546 202	536 892
0.0006	536 919	527 426
0.0007	528 924	519 274
0.0008	521 887	512 099
0.0009	515 594	505 684
0.001	509 895	499 874
0.002	470 710	459 949
0.003	446 375	435 175
0.004	428 450	416 942
0.005	414 160	402 417
0.006	402 231	390 300
0.007	391 965	379 879
0.008	382 937	370 721
0.009	374 872	362 543
0.010	367 573	355 148
0.015	338 759	325 995
0.020	317 620	304 662
0.025	300 836	287 763
0.030	286 880	273 743
0.035	274 918	261 745
0.040	264 442	251 260
0.045	255 119	241 944
0.050	246 716	233 563
0.055	239 069	225 948
0.060	232 051	218 970
0.065	225 568	212 534
0.070	219 544	206 562
0.075	213 920	200 994
0.080	208 645	195 780
0.085	203 682	190 880
0.090	198 994	186 259
0.095	194 555	181 888
0.10	190 340	177 743
0.15	157 036	145 186
0.20	133 688	122 596
0.25	115 969	105 655
0.30	101 887	092 207
0.35	090 348	081 308
0.40	080 688	072 243
0.45	072 470	064 577
0.50	065 389	058 010
0.55	059 229	052 344
0.60	053 825	047 365
0.65	049 052	043 004
0.70	044 813	039 148
0.75	041 029	035 721
0.80	037 636	032 660
0.85	034 585	029 919
0.90	031 830	027 453
0.95	029 335	025 228
1.0	027 070	023 215
1.1	023 132	019 732
1.2	019 845	016 844
1.3	017 084	014 432

* Accuracy of values for $\eta = 4.0$ is dubious. See text.

TABLE 1. The functions $C_{1/7}$ and $F_{1/7}$.—*Continued.*

η	$C_{1/7}$	$F_{1/7}$
1.4	014 752	012 406
1.5	012 771	010 694
1.6	011 082	009 242
1.7	009 637	008 005
1.8	008 395	006 948
1.9	007 326	006 041
2.0	006 404	005 262
2.5	003 329	002 693
3.0	001 773	001 415
4.0	000 529*	000 413*
5.0	000 164	000 125
6.0	000 0523	000 0394
7.0	000 0171	000 0127
8.0	000 0056	000 0042
9.0	000 0019	000 0014
10.0	000 0006	000 0005

equation:

$$C_m(\eta) = 1 - I\left(\eta, -\frac{1+m}{1+2m}\right). \tag{17}$$

Thus, equation (16A) may be written as

$$\theta = C_m(\eta). \tag{18}$$

We now investigate the distribution of the vertical flux of the diffusing entity, ϕ:

$$\phi = -K\frac{\partial\theta}{\partial z} = -K\frac{d\theta}{d\eta}\cdot\frac{\partial\eta}{\partial z}, \tag{19}$$

so that it follows from equations (4), (10), and (16) that

$$\phi(\eta, x) = \phi(0, x)e^{-\eta}. \tag{20}$$

Here, $\phi(0, x)$ is the flux at the surface $z = 0$ ($\eta = 0$) and has the following value:

$$\phi(0,x) = \frac{(2+m-n)K_1}{\Gamma\left(\dfrac{1-n}{2+m-n}\right)} \cdot \left(\frac{(2+m-n)^2K_1x}{u_1}\right)^{-(1-n)/(2+m-n)} \tag{21}$$

$$\phi(0,x) = \frac{(1+2m)K_1}{\Gamma\left(\dfrac{m}{1+2m}\right)} \cdot \left(\frac{(1+2m)^2K_1x}{u_1}\right)^{-m/(1+2m)} \tag{21A}$$

$$\phi(0,x) = \frac{9K_1}{7\Gamma(1/9)} \cdot \left(\frac{81K_1x}{49u_1}\right)^{-1/9}. \tag{21B}$$

6. Two-dimensional diffusion: flux boundary condition

We now proceed to the solution of (2), (3), and (4) subject to (8). We may rewrite (2) in terms of ϕ (*i.e.*, as a continuity equation) in the form

$$\frac{\partial\theta}{\partial x} = -\frac{1}{u}\frac{\partial\phi}{\partial z}. \tag{22}$$

Differentiating with respect to z,

$$\frac{\partial^2\theta}{\partial x\partial z} = -\frac{\partial}{\partial z}\left(\frac{1}{u}\frac{\partial\phi}{\partial z}\right), \tag{23}$$

which we may rewrite, using (19) and the fact that K is a function of z only, as

$$\frac{1}{K}\frac{\partial\phi}{\partial x} = \frac{\partial}{\partial z}\left(\frac{1}{u}\frac{\partial\phi}{\partial z}\right). \tag{24}$$

Equation (24) evidently describes the "diffusion" of ϕ. The conditions governing (24) are found from (8) to be:

$$\left.\begin{array}{lll} x = 0, & z > 0, & \phi = 0 \\ x \geqslant 0, & z = 0, & \phi = 1 \end{array}\right\}. \tag{25}$$

It will be seen that we have reduced the present problem to a form identical to that solved in section 5, except that we must now replace m by $-n$, n by $-m$, u_1 by K_1^{-1}, and K_1 by u_1^{-1}. Substitution (10) is again appropriate, and the solution is

$$\phi = 1 - I\left(\eta, -\frac{1-n}{2+m-n}\right). \tag{26}$$

This solution is valid for

$$2 + m - n > 0; \quad m > -1. \tag{27}$$

Neither of these restrictions is of importance in meteorological applications.[8]

Equations (4), (10), (19), and (26) now yield

$$\frac{d\theta}{d\eta} = -\frac{1}{(2+m-n)K_1}\left(\frac{(2+m-n)^2K_1x}{u_1}\right)^{(1-n)/(2+m-n)} \times \eta^{-(1+m)/(2+m-n)}\left[1-I\left(\eta, -\frac{1-n}{2+m-n}\right)\right]. \tag{28}$$

Integration by parts gives

$$\theta(\eta, x) = \frac{1}{(1-n)\Gamma\left(\frac{1+m}{2+m-n}\right)K_1} \times \left(\frac{(2+m-n)^2K_1x}{u_1}\right)^{(1-n)/(2+m-n)} \times \left[e^{-\eta} - \Gamma\left(\frac{1+m}{2+m-n}\right)\eta^{(1-n)/(2+m-n)} \times \left\{1 - I\left(\eta, -\frac{1-n}{2+m-n}\right)\right\}\right]. \tag{29}$$

The limits of this integration depend on the result that conditions (8) imply the further condition

$$x \geqslant 0, \quad z \to \infty, \quad \theta \to 0. \tag{30}$$

[8] In contrast to the case of the concentration boundary condition, we can here obtain a solution for $n = 1$. In practice, $m > 0$, so that solutions for n at least as great as 2 are possible.

Equation (29) also makes use of the result that

$$\lim_{\eta\to\infty}\left[\eta^{(1-n)/(2+m-n)}\left\{1-I\left(\eta, -\frac{1-n}{2+m+n}\right)\right\}\right]=0, \tag{31}$$

which follows very simply from the asymptotic expansion of $1 - I$ for large η. Compare Appendix 1.

Equation (29) is obviously of the form

$$\theta(\eta, x) = \theta(0, x)\cdot F\left(\eta, \frac{2+m-n}{1-n}\right), \tag{32}$$

where

$$\theta(0, x) = \frac{1}{(1-n)\Gamma\left(\frac{1+m}{2+m-n}\right)K_1} \times \left(\frac{(2+m-n)^2K_1x}{u_1}\right)^{(1-n)/(2+m-n)} \tag{33}$$

$$\theta(0, x) = \frac{1}{m\Gamma\left(\frac{1+m}{1+2m}\right)K_1}\left(\frac{(1+2m)^2K_1x}{u_1}\right)^{m/(1+2m)} \tag{33A}$$

$$\theta(0, x) = \frac{7}{\Gamma(8/9)K_1}\left(\frac{81K_1x}{49u_1}\right)^{1/9} \tag{33B}$$

and

$$F(\eta, \beta) = e^{-\eta} - \Gamma\left(1-\frac{1}{\beta}\right)\eta^{1/\beta}\left[1-I\left(\eta, -\frac{1}{\beta}\right)\right]. \tag{34}$$

For the case $n = 1 - m$, it is convenient to introduce the notation $F_m(\eta)$ to denote $F[\eta, 2 + 1/m]$. In this case, we may therefore write

$$\theta(\eta, x) = \theta(0, x)\cdot F_m(\eta). \tag{35}$$

The properties of F_m, and its calculation, are treated in Appendix 2. $F_{1/7}$ is tabulated in table 1 and graphed in figs. 4 and 5.

7. Two-dimensional diffusion: radiation boundary condition

Our method of solution of (2), (3), and (4) subject to (9) is to find a suitable linear combination of the solutions of sections 5 and 6 which satisfies (9) to a reasonable accuracy. A more elaborate method of superposition would, doubtless, enable (9) to be satisfied to any desired accuracy. However, the present method has the merit of simplicity and yields results to an accuracy which is almost certainly adequate in the practical applications. Essentially, our method relies on the fact that the quantity $x^\gamma + x^{-\gamma}$, where γ is a small positive number, varies only slowly as x varies through several orders of magnitude centered on $x = 1$.

From section 5, as part of the solution of (2), (3), and (4) subject to

$$\left.\begin{array}{lll} x = 0, & z > 0, & \theta = 0 \\ x \geqslant 0, & z = 0, & \theta = a \end{array}\right\}, \tag{36}$$

we have

$$\phi_0 = a \cdot \frac{2+m-n}{\Gamma\left(\dfrac{1-n}{1+m-n}\right)} \cdot X^{-1}, \tag{37}$$

where

$$X = \frac{1}{K_1}\left(\frac{(2+m-n)^2 K_1 x}{u_1}\right)^{(1-n)/(2+m-n)}. \tag{38}$$

Also, from section 6, as part of the solution of (2), (3), and (4) subject to

$$\left.\begin{array}{lll} x = 0, & z > 0, & \theta = 0 \\ x \geqslant 0, & z = 0, & \phi = b \end{array}\right\}, \tag{39}$$

we have

$$\theta_0 = \frac{bX}{(1-n)\Gamma\left(\dfrac{1+m}{2+m-n}\right)}. \tag{40}$$

Superposing the two solutions, we obtain

$$\theta_0 = a + \frac{bX}{(1-n)\Gamma\left(\dfrac{1+m}{2+m-n}\right)};$$

$$\phi_0 = a\frac{2+m-n}{\Gamma\left(\dfrac{1-n}{2+m-n}\right)} \cdot X^{-1} + b. \tag{41}$$

We note, now, that in order to satisfy (9) by this superposed solution, we should require that

$$\alpha a + \frac{\alpha b X}{(1-n)\Gamma\left(\dfrac{1+m}{2+m-n}\right)} + (1-\alpha)a \cdot \frac{2+m-n}{\Gamma\left(\dfrac{1-n}{2+m-n}\right)} \cdot X^{-1} + (1-\alpha)b = 1. \tag{42}$$

Evidently, (42) cannot in general be satisfied exactly, since X is not a constant. However, we are free to choose the constants a and b in such a way that the deviations from (42) are minimal in the range of X of interest. For this to be so, the terms in X and X^{-1} must be equal when X assumes the value $\bar{X}$, which is the geometrical mean of the range of X-values of interest. Thus, if we wish to study the x-range 10 to 10^7 cm, the appropriate value of $\bar{X}$ is the value obtained for X in (38) with $x = \bar{x} = 10^4$.

We then have

$$\frac{a}{b} = \frac{\alpha}{1-\alpha} \frac{\Gamma\left(\dfrac{1-n}{2+m-n}\right)}{\Gamma\left(\dfrac{1+m}{2+m-n}\right)} \cdot \frac{\bar{X}^2}{(1-n)(2+m-n)}. \tag{43}$$

We could then proceed by satisfying (42) exactly at $x = \bar{x}$, and using (42) and (43) to evaluate a and b. In the cases where $0 < \alpha < 1$, which are of greatest interest to us here, this would produce a systematic error in the satisfaction of the boundary condition, the deviations both as x increases, and as x decreases, from the value $\bar{x}$ being in the same sense. A preferable procedure is to match the boundary condition in such a way that the *integrated* error in fitting the boundary condition is zero over some appropriate region, say from $x = 0$ to $x = x_1$. Thus, for our numerical example, it would be suitable to take $x_1 = 10^6$. The equation to be used in conjunction with (43) for evaluating a and b is then

$$\alpha a + \frac{2c\alpha b\bar{X}}{(1-n)\Gamma\left(\dfrac{1+m}{2+m-n}\right)} + (1-\alpha)b = 1, \tag{44}$$

where c is a factor of order-of-magnitude unity and is given by

$$c = \frac{\bar{x}}{2x_1}\int_0^{x_1/\bar{x}} (y^{\gamma}+y^{-\gamma})dy = \frac{1}{2}\left[\frac{(x_1/\bar{x})^{\gamma}}{1+\gamma} + \frac{(x_1/\bar{x})^{-\gamma}}{1-\gamma}\right] \tag{45}$$

with

$$\gamma = (1-n)/(2+m-n). \tag{46}$$

For $\bar{x} = 10^4$ cm, $x_1 = 10^6$ cm, $m = 1 - n = 1/7$, $c = 1.0879$.

The expressions finally obtained for a and b are

$$a = \frac{\alpha\Gamma\left(\dfrac{1-n}{2+m-n}\right)\bar{X}^2}{\alpha^2\Gamma\left(\dfrac{1-n}{2+m-n}\right)\bar{X}^2 + 2c\alpha(1-\alpha)(2+m-n)\bar{X} + (1-\alpha)^2\Gamma\left(\dfrac{1+m}{2+m-n}\right)(1-n)(2+m-n)} \tag{47}$$

$$b = \frac{(1-\alpha)\Gamma\left(\frac{1+m}{2+m-n}\right)(1-n)(2+m-n)}{\alpha^2\Gamma\left(\frac{1-n}{2+m-n}\right)\bar{X}^2+2c\alpha(1-\alpha)(2+m-n)\bar{X}+(1-\alpha)^2\Gamma\left(\frac{1+m}{2+m-n}\right)(1-n)(2+m-n)}. \tag{48}$$

With a and b evaluated, the solution is effectively complete. The required result is now the appropriate linear combination of the solutions developed in sections 5 and 6.

Accuracy of the approximation. The error in the satisfaction of the boundary condition

$$\alpha\theta_0 + (1-\alpha)\phi_0 = 1 \tag{49}$$

is found to be of the form

$$f_1(\alpha)\cdot f_2(x) \tag{50}$$

where

$$f_1(\alpha) = \alpha a + (1-\alpha)b - 1 = \frac{2c\alpha(1-\alpha)(2+m-n)\bar{X}}{\alpha^2\Gamma\left(\frac{1-n}{2+m-n}\right)\bar{X}^2+2c\alpha(1-\alpha)(2+m-n)\bar{X}+(1-\alpha)^2\Gamma\left(\frac{1+m}{2+m-n}\right)(1-n)(2+m-n)} \tag{51}$$

and

$$f_2(x) = 1 - \frac{1}{2c}\left[\frac{X}{\bar{X}} + \frac{\bar{X}}{X}\right]. \tag{52}$$

That is, the accuracy of the approximation depends both on the value of α and the x-range we wish to investigate. We may examine these functions by assigning numerical values. We use the values $u_1 = 179$, $K_1 = 19.3$, and the m, n, $\bar{x}$ and x_1 values used above. These values are typical of those which enter the later practical applications. For these values,

$$f_1(\alpha) = \frac{\alpha(1-\alpha)}{0.703 - 0.407\alpha + 0.133\alpha^2}. \tag{53}$$

This function is plotted in fig. 1. Provided $-0.3 < \alpha < 1.1$, f_2 tends to be small, and we may regard the present method as applicable. Fortunately, α-values arising in the practical applications tend to lie in the range 0 to 1 and, in particular, to assume values close to 0 or to 1, so that the present method proves to be quite suitable.

Also, for this case,

$$f_2(x) = 1 - \frac{1}{2.1758}\left[\left(\frac{x}{10^4}\right)^{1/9} + \left(\frac{x}{10^4}\right)^{-1/9}\right]. \tag{54}$$

Note that f_2 is independent of the adopted values of u_1 and K_1. This f_2 function is shown in fig. 2.

The magnitude of the errors of the method are then readily illustrated with the aid of figs. 1 and 2. Thus, for the worst case with $-0.3 < \alpha < 1.1$, $\alpha \approx 0.56$, $f_1(\alpha) \approx 0.48$, the errors at $x = 10^4$; 10^3 and 10^5; 10^2 and 10^6; 10 and 10^7 are respectively: -3.9 per cent; -2.4 per cent; $+2.0$ per cent; $+9.7$ per cent. The typical values $\alpha = 0.1$, $f_1(\alpha) = 0.136$ yield the following corresponding errors: -1.1 per cent; -0.7 per cent; $+0.6$ per cent; $+2.8$ per cent.

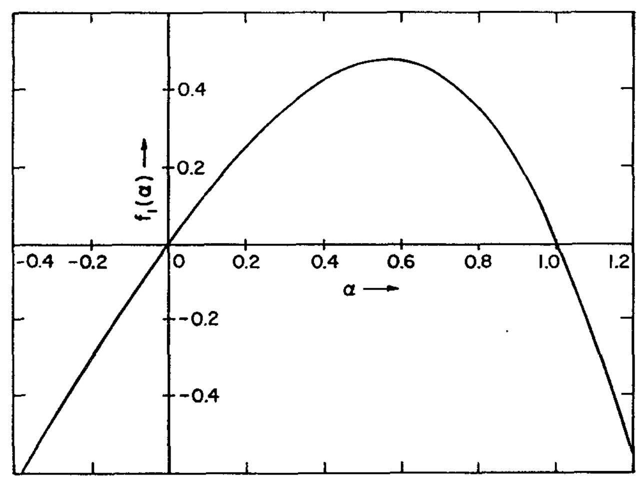

FIG. 1. The function $f_1(\alpha)$ for the numerical values given in the text. The error in fitting the radiation boundary condition is equal to $f_1(\alpha)\cdot f_2(x)$.

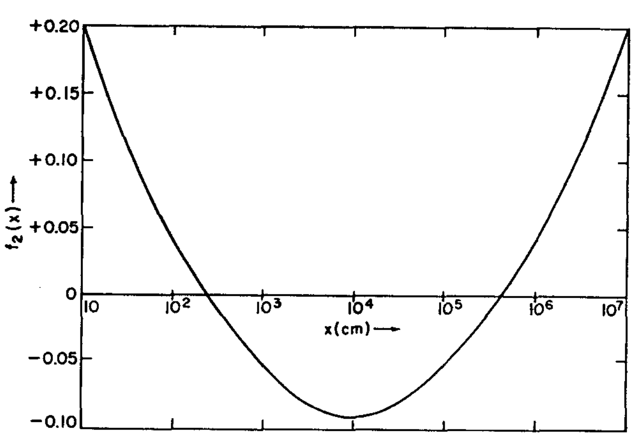

FIG. 2. The function $f_2(x)$ for the numerical values given in the text. The error in fitting the radiation boundary condition is equal to $f_1(\alpha)\cdot f_2(x)$.

It is evident that, as long as α lies in the range specified above, the present method yields results of sufficient accuracy over an x-range large enough for micrometeorological purposes.

8. The theory of advective inversion

We may develop the quantitative theory of advective inversion by superposing on the preceding results a steady vertical flux of the diffusing entity, ϕ_{00}, which is supposed to occur uniformly, both upwind and downwind of $x = 0$. We have

$$\phi_{00} = \frac{K_1(1-n)}{10^{4(1-n)}} \cdot \Delta_z\theta, \tag{55}$$

where $\Delta_z\theta$ denotes the difference in θ (over the regions upwind of $x = 0$) between the surface and 10^4 cm.[9] We shall here assume that $K(z)$ is the same for both the upwind and downwind regions. The validity of this assumption will be discussed later in this series.

Advective inversion with concentration boundary condition. We shall show in a later paper that, although the boundary conditions for most advection problems of interest are of the radiation type, they tend to approach closely either the concentration type or the flux type. Concentration-like advective effects lead to the type of advective inversion which is of greatest practical and theoretical importance. We may study this case adequately by investigating the case where the downwind boundary condition is purely of the concentration type.

We here define an inversion surface as one at which

$$\frac{\partial\theta}{\partial z} = 0; \quad \frac{\partial^2\theta}{\partial z^2} < 0. \tag{56}$$

We denote by $\Delta\theta_0$ the difference between values of θ at $z = 0$ upwind and downwind of $x = 0$. The condition that an inversion (not present upwind) exists is that both $\Delta_z\theta$ and $\Delta\theta_0$ be positive. From section 5, we then have, on the inversion surface,

$$e^{\eta} = \frac{10^{4(1-n)}}{\Gamma\left(\dfrac{3+m-2n}{2+m-n}\right)} \times\left((2+m-n)^2\frac{K_1}{u_1}x\right)^{-(1-m)/(2+m-n)} \cdot \frac{\Delta\theta_0}{\Delta_z\theta}. \tag{57}$$

The maximum downwind extent of the inversion, $x = x_{\max}$, occurs at the intersection of the inversion surface and $z = 0$. That is, we put $\eta = 0$ in (57), obtaining

$$x_{\max} = \frac{u_1}{K_1(2+m-n)^2}\left[\frac{10^4}{\Gamma\left(\dfrac{3+m-2n}{2+m-n}\right)^{1/(1-n)}}\right]^{2+m-n} \times\left(\frac{\Delta\theta_0}{\Delta_z\theta}\right)^{(2+m-n)/(1-n)} \tag{58}$$

$$x_{\max} = \frac{u_1}{K_1(1+2m)^2}\left[\frac{10^4}{\Gamma\left(\dfrac{1+3m}{1+2m}\right)^{1/m}}\right]^{1+2m} \times\left(\frac{\Delta\theta_0}{\Delta_z\theta}\right)^{2+1/m} \tag{58A}$$

$$x_{\max} = \frac{49u_1}{81K_1} \cdot \frac{10^{36/7}}{\left[\Gamma\left(\dfrac{10}{9}\right)\right]^9} \cdot \left(\frac{\Delta\theta_0}{\Delta_z\theta}\right)^9. \tag{58B}$$

That is, for the numerical value $K_1/u_1 = 0.108$ cm$^{2/7}$ which we have occasion to use in later work, (58B) becomes

$$x_{\max} = 1.27 \times 10^6 \left(\frac{\Delta\theta_0}{\Delta_z\theta}\right)^9. \tag{59}$$

Note that these results depend on u_1 and K_1 only through the quantity K_1/u_1 which, at least under near-neutral conditions, is virtually independent of wind strength.

Evidently the extent of the inversion depends very critically on the ratio $\Delta\theta_0/\Delta_z\theta$. This ratio, which is found in the practical applications to lie within fairly well-defined limits, will be discussed further in a later paper of this series.

Further manipulations involving (57) and (58) yield the following equation of the inversion surface:

$$z = \left[\frac{(1-n)(2+m-n)K_1}{u_1} x \log\frac{x_{\max}}{x}\right]^{1/(2+m-n)}. \tag{60}$$

This may be put in the dimensionless form

$$\zeta = \left[\chi \log\frac{1}{\chi}\right]^{1/(2+m-n)} \tag{61}$$

$$\zeta = \left[\chi \log\frac{1}{\chi}\right]^{1/(1+2m)} \tag{61A}$$

$$\zeta = \left[\chi \log\frac{1}{\chi}\right]^{7/9} \tag{61B}$$

where

$$\zeta = \left(\frac{2+m-n}{1-n}\right)^{1/(2+m-n)} \cdot \frac{\Gamma\left(\dfrac{3+m-2n}{2+m-n}\right)}{10^4} \times\left(\frac{\Delta\theta_0}{\Delta_z\theta}\right)^{-1/(1-n)} \cdot z \tag{62}$$

[9] The theory could be developed similarly for any other reference height, the value of 10^4 cm being quite arbitrary.

$$\zeta=\left(2+\frac{1}{m}\right)^{1/(1+2m)}\cdot\frac{\Gamma\left(\frac{1+3m}{1+2m}\right)}{10^4}\cdot\left(\frac{\Delta\theta_0}{\Delta_z\theta}\right)^{-1/m}\cdot z \quad (62A)$$

$$\zeta=\left(\frac{15}{7}\right)^{7/9}\cdot\frac{\Gamma\left(\frac{10}{9}\right)}{10^4}\cdot\left(\frac{\Delta\theta_0}{\Delta_z\theta}\right)^{-7}\cdot z$$

$$=1.71\times10^{-4}\left(\frac{\Delta\theta_0}{\Delta_z\theta}\right)^{-7}\cdot z \quad (62B)$$

and

$$\chi = x/x_{\max}. \quad (63)$$

Note that ζ is dimensionless since the 10^4 in the denominator of (62) represents the reference height 10^4 cm and has the dimension of length.

The $\zeta(\chi)$ function of (61B) is shown in fig. 3. It illustrates the general form of advective inversions of this nature.

It is simply shown by differentiation that the maximum height of the inversion, $z_{\max}$, occurs at

$$x = x_{\max}/e, \quad (64)$$

and that

$$z_{\max} = \left(\frac{1-n}{(2+m-n)e}\right)^{1/(2+m-n)} \times \frac{10^4}{\Gamma\left(\frac{3+m-2n}{2+m-n}\right)}\cdot\left(\frac{\Delta\theta_0}{\Delta_z\theta}\right)^{(1/1-n)} \quad (65)$$

$$z_{\max} = \left(\frac{m}{(1+2m)e}\right)^{1/(1+2m)} \cdot\frac{10^4}{\Gamma\left(\frac{1+3m}{1+2m}\right)}\cdot\left(\frac{\Delta\theta_0}{\Delta_z\theta}\right)^{1/m} \quad (65A)$$

$$z_{\max} = (9e)^{-7/9}\frac{10^4}{\Gamma\left(\frac{10}{9}\right)}\cdot\left(\frac{\Delta\theta_0}{\Delta_z\theta}\right)^7$$

$$= 0.09\times10^4\left(\frac{\Delta\theta_0}{\Delta_z\theta}\right)^7. \quad (65B)$$

The expressions for ζ and $z_{\max}$ are independent of K_1 and u_1. That is, for constant values of m, n and $\Delta\theta_0/\Delta_z\theta$, the vertical scale of the inversion, and its maximum height, are independent of wind strength and surface roughness.

We note here again the extreme sensitivity of the properties of the inversion to the ratio $\Delta\theta_0/\Delta_z\theta$.

Advective inversion with flux boundary condition. This case is discussed only for the sake of completeness. It will be shown later in this series that this form of

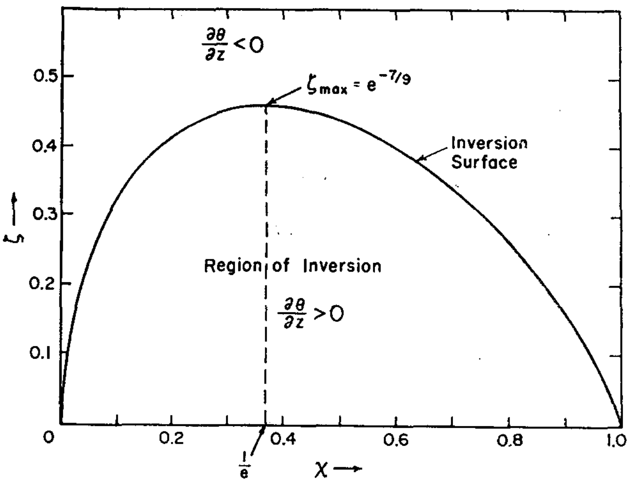

FIG. 3. Advective inversion (concentration type) for the case $m = 1 - n = 1/7$. The inversion surface is plotted in the dimensionless form $\zeta(\chi)$.

inversion is most unlikely to occur in practice. We consider the situation where the upwind flux is again ϕ_{00} at all levels and the downwind boundary condition is that the flux at $z = 0$ has the constant value $\phi_{00} - \Delta\phi_0$. Obviously, an inversion (not present upwind) develops only when $\Delta\phi_0 > \phi_{00} > 0$. In this case, the equation of the inversion surface is, from section 6,

$$I\left(\eta, -\frac{1-n}{2+m-n}\right) = 1 - \phi_{00}/\Delta\phi_0. \quad (66)$$

The inversion surface is a surface of constant η, the η-value, and thus the relative height of the inversion, being determined by $\phi_{00}/\Delta\phi_0$. The equation of the inversion surface clearly reduces to the form

$$z \propto x^{1/(2+m-n)} \quad (67)$$

$$z \propto x^{1/(1+2m)} \quad (67A)$$

$$z \propto x^{7/9}. \quad (67B)$$

This type of advective inversion is quite dissimilar to the concentration type. It extends downwind indefinitely and exhibits no maximum height.

9. Conclusion

The aim of the present paper has been to present the basic methods of analysis to be used in this study of the theory of local advection. We defer application of the methods to specific problems, the presentation of illustrative numerical examples, and critical discussion of the assumptions on which the analysis is based to later papers in this series.

REFERENCES

Calder, K. L., 1949: Eddy diffusion and evaporation in flow over aerodynamically smooth and rough surfaces: a treatment based on laboratory laws of turbulent flow with special reference to conditions in the lower atmosphere. *Quart. J. Mech. appl. Math.*, **2**, 153–176.

Carslaw, H. S., and J. C. Jaeger, 1947: *Conduction of heat in solids.* Oxford, Clarendon Press, 386 pp.

Deacon, E. L., C. H. B. Priestley, and W. C. Swinbank, 1958: Evaporation and the water balance. *Arid Zone Research-X: Climatology, Reviews of Research*, Paris, UNESCO, 9–34.

Frost, R., 1946: Turbulence and diffusion in the lower atmosphere. *Proc. r. Soc. London*, A, **186**, 20–35.

Pasquill, F., 1943: Evaporation from a plane, free-liquid surface into a turbulent air stream. *Proc. r. Soc. London*, A, **182**, 75–95.

Pearson, K., 1951: *Tables of the incomplete Γ-function.* Cambridge University Press, 164 pp.

Philip, J. R., 1957. Evaporation, and moisture and heat fields in the soil. *J. Meteor.*, **14**, 354–366.

Priestley, C. H. B., 1951: Meteorological aspects of soil and crop evaporation. *Proc. Specialist Conf. in Agr.* (Australia, 1949), 35–42.

Sutton, O. G., 1953. *Micrometeorology.* New York, McGraw-Hill, 333 pp.

Whittaker, E. T., and G. N. Watson, 1927: *A course of modern analysis.* Cambridge University Press, pp. 608.

Yih, C.-S., 1952: On a differential equation of atmospheric diffusion. *Trans. Amer. geophys. Union*, **33**, 8–12.

APPENDIX 1

The function C_m, its properties and its computation.

Using the Taylor expansion of $e^{-\eta}$ in (15), we obtain

$$\theta = 1 - \frac{\eta^{1/\beta}}{\Gamma\left(\dfrac{\beta+1}{\beta}\right)}\left\{1 - \frac{\eta}{\beta+1} + \frac{\eta^2}{2!(2\beta+1)} - \frac{\eta^3}{3!(3\beta+1)} + \frac{\eta^4}{4!(4\beta+1)} - \cdots\right\} \quad (68)$$

where

$$\beta = \frac{2+m-n}{1-n} \quad (69)$$

$$\beta = 2 + \frac{1}{m} \quad (69\text{A})$$

$$\beta = 9. \quad (69\text{B})$$

For m and n values of interest, the series in the curly bracket of (68) converges rapidly for a large part of the η-range, so that (68) is very suitable for numerical computation. In particular, the use of (69A) in (68) yields a simple method of computing C_m. We have used this method to compute $C_{1/7}$ in the range $0 \leqslant \eta \leqslant 3$, the results being given in table 1. We give only illustrative values for $\eta < 10^{-6}$; fuller tabulation is unnecessary, since for small values of η we may use the very good approximation, derived from (68), that

$$C_m \approx 1 - \eta^{m/(1+2m)} \Big/ \Gamma\left(\frac{1+3m}{1+2m}\right). \quad (70)$$

For large η, we may use the asymptotic expansion of (15),

$$\theta = \frac{e^{-\eta}}{\Gamma\left(\dfrac{1}{\beta}\right)\eta^{1-1/\beta}}\left\{1 - \frac{\beta-1}{\beta\eta} + \frac{(\beta-1)(2\beta-1)}{(\beta\eta)^2} - \frac{(\beta-1)(2\beta-1)(3\beta-1)}{(\beta\eta)^3} + \cdots\right\}, \quad (71)$$

where β is again specified by (69). We have used (71) to compute the values of $C_{1/7}$ for $\eta \geqslant 4$ shown in table 1.

The error in the table of $C_{1/7}$ should not exceed one in the last figure given, additional decimals having been retained in the computation. However, we note an exception at $\eta = 4$, which arises because (71) cannot yield sufficient accuracy for η-values as small as this. Comparison of the present results with the short four-decimal table of $C_{1/7}$ given by Frost (1946) reveals a number of instances where Frost's result is apparently incorrect by one unit in the fourth decimal and two instances where the discrepancy in the fourth decimal is two.

The following asymptotic properties of C_m follow from (68) and (71):

$$\begin{aligned}\lim_{\eta\to 0} C_m &= 1 - \eta^{m/(1+2m)} \Big/ \Gamma\left(\frac{1+3m}{1+2m}\right) \\ \lim_{\eta\to\infty} C_m &= e^{-\eta} \Big/ \Gamma\left(\frac{m}{1+2m}\right)\eta^{(1+m)/(1+2m)}.\end{aligned} \quad (72)$$

These properties of C_m are reflected in the plots of $C_{1/7}$ shown in figs. 4 and 5. Fig. 4 shows $C_{1/7}$ (η) plotted with the scales of η and $(1 - C_{1/7})$ logarithmic, while in fig. 5 the scale of η is linear and that of $C_{1/7}$ logarithmic.

We have here dealt specifically with the function C_m; however, it will be evident that the results apply also with little or no modification to the Pearson I-function.

APPENDIX 2

The function F_m, its properties and its computation.

Use of the Taylor expansion of $e^{-\eta}$ leads to the following series form of equation (34):

$$F(\eta,\beta) = 1 - \Gamma\left(1-\frac{1}{\beta}\right)\cdot\eta^{1/\beta} + \frac{\eta}{\beta-1} - \frac{\eta^2}{2!(2\beta-1)} + \frac{\eta^3}{3!(3\beta-1)} - \frac{\eta^4}{4!(4\beta-1)} + \cdots. \quad (73)$$

For m- and n-values of interest, this series converges rapidly over most of the relevant η-range, so

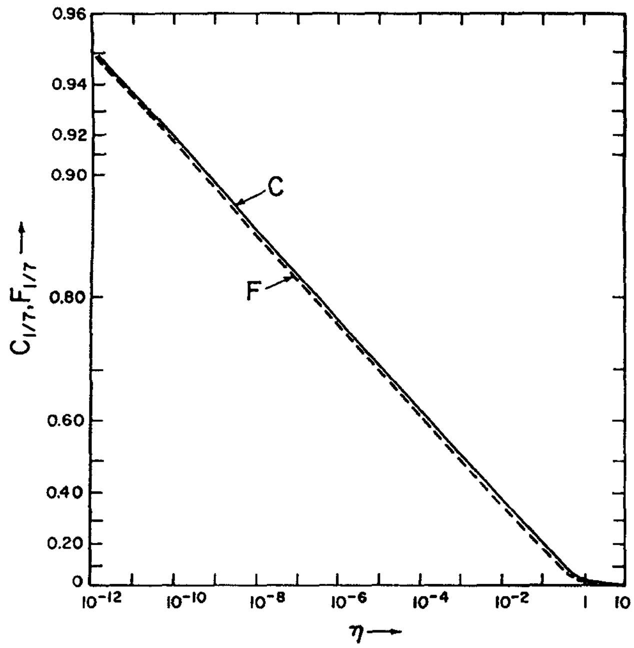

FIG. 4. The functions $C_{1/7}$ and $F_{1/7}$. Scales of $(1 - C_{1/7})$ and $(1 - F_{1/7})$, and of η, logarithmic.

that (73), like (68), is very suitable for numerical computation.

We have used (73) to compute $F_{1/7}$ in the range $0 \leqslant \eta \leqslant 3$, the results being given in table 1. We give only illustrative values for $\eta < 10^{-6}$, fuller tabulation being unnecessary, since, for small values of η, we have to have a very good approximation

$$F_m \approx 1 - \Gamma\left(\frac{1+m}{1+2m}\right)\eta^{m/(1+2m)}. \tag{74}$$

Also, for large η, we may use the asymptotic expansion of equation (34), which is

$$F(\eta,\beta) = \frac{e^{-\eta}}{\beta\eta}\left\{1 - \frac{\beta+1}{\beta\eta} + \frac{(\beta+1)(2\beta+1)}{(\beta\eta)^2} - \frac{(\beta+1)(2\beta+1)(3\beta+1)}{(\beta\eta)^3} + \cdots\right\}. \tag{75}$$

We have used (75) to compute the values of $F_{1/7}$ for $\eta \geqslant 4$ shown in table 1. The accuracy of the table of $F_{1/7}$ follows closely that of the $C_{1/7}$ table. Once again, the value at $\eta = 4$ is of uncertain accuracy, due to the use of asymptotic expansion (75) for this relatively small value of η.

The following asymptotic properties of F_m follow from (73) and (75) and are reflected in the plots of $F_{1/7}$ shown in figs. 4 and 5:

$$\begin{aligned} \lim_{\eta\to 0} F_m &= 1 - \Gamma\left(\frac{1+m}{1+2m}\right)\cdot\eta^{m/(1+2m)} \\ \lim_{\eta\to\infty} F_m &= e^{-\eta}\Big/\frac{1+2m}{m}\cdot\eta. \end{aligned} \tag{76}$$

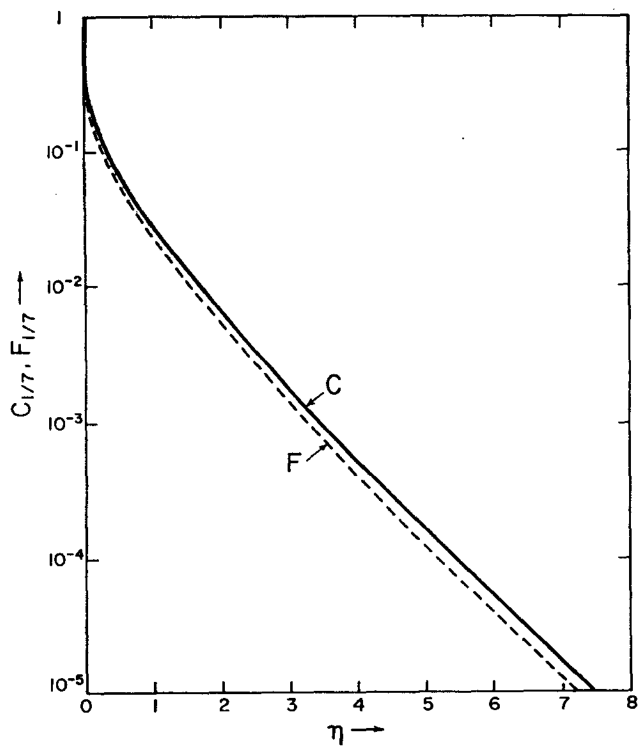

FIG. 5. The functions $C_{1/7}$ and $F_{1/7}$. Scale of $C_{1/7}$ and $F_{1/7}$ logarithmic; scale of η linear.

The general similarity of the power series and asymptotic expansions of C_m and F_m will be noted, as well as the very similar behavior and nearness of values of $C_{1/7}$ and $F_{1/7}$. We have the following results from (72) and (76):

$$\lim_{\eta\to 0}(F_m/C_m) = \frac{1-\Gamma\left(\dfrac{1+m}{1+2m}\right)\eta^{m/(1+2m)}}{1-\dfrac{\eta^{m/(1+2m)}}{\Gamma\left(\dfrac{1+3m}{1+2m}\right)}}$$

$$\approx 1 - \frac{\pi^2}{6}\left(\frac{m}{1+2m}\right)^2\Gamma\left(\frac{1+m}{1+2m}\right)\eta^{m/(1+2m)}$$

$$\lim_{\eta\to\infty}(F_m/C_m) = \Gamma\left(\frac{1+3m}{1+2m}\right)\eta^{-m/(1+2m)}. \tag{77}$$

Neither of these limits will vary much from unity in the m- and η-ranges of interest. We have the further result that

$$\lim_{m\to 0}(F_m/C_m) = 1. \tag{78}$$

That is, when m is small, as it will usually be, F_m and C_m will not differ greatly from each other throughout the whole η-range. This leads to the conclusion that, in any practical applications of advection theory, it may be sufficiently accurate to put $F_m \approx C_m$, thus simplifying the formulation and enabling the required solutions to be obtained solely from tabulations of C_m.

We have dealt here specifically with the function F_m; however, it will be evident that similar results hold for the function $F(\eta, \beta)$. The treatment of the ratio F_m/C_m has, as its more general counterpart, treatment of the ratio $F(\eta, \beta)/[1 - I(\eta, (1 - \beta)/\beta]$.